Theory of the Hydrogen Maser*

DANIEL KLEPPNER, H. MARK GOLDENBERG, AND NORMAN F. RAMSEY
Harvard University, Cambridge, Massachusetts

(Received December 15, 1961)

The behavior of the atomic hydrogen maser is analyzed for both stationary and transient operation. An expression for noise in the signal from the maser oscillator is derived by applying the previously developed theory of Shimoda, Wang, and Townes. A variety of relaxation phenomena are analyzed, including effects of chemical reaction with the surface and magnetic field inhomogeneities. Several mechanisms leading to frequency shifts in the maser are also analyzed, including cavity pulling and the Doppler effect.

I. INTRODUCTION

MOST attempts to observe radiofrequency or microwave spectral lines with high precision incorporate one or more of the following features: (a) observation of the resonance over a relatively long period of time in order to obtain a narrow resonance line; (b) observation of a spectral line which is as pure as possible so that there is no broadening due to different components of the line or to the environment of the atom or molecule concerned; (c) a technique for eliminating, or at least greatly reducing, the first-order Doppler shift; and (d) a means for obtaining a favorable signal-to-noise ratio such as is provided in the low-noise amplification which characterizes a maser oscillator.

Although most high-precision radiofrequency and microwave experiments depend upon one or more of the above characteristics, none of them in the past has attained high quality in all of these features in a single method. Atomic beam hyperfine structure resonance experiments are excellent with regard to purity of the spectral line, but the atoms have only moderately long lifetimes. The original ammonia maser was excellent with regard to signal-to-noise ratio but had only a short lifetime and used a complicated spectral line. Solid state masers are good with respect to all the criteria except for broadening of the lines by the influence of neighboring atoms in the material. Optical pumping experiments with buffer gases are excellent in every point except for the effects of perturbations due to the frequent collisions of the radiating atoms with the atoms of the buffer gas.

The hydrogen maser experiments described in the present paper originated in an effort to obtain a single device which was highly favorable in all of these features. Historically, the experiments were an outgrowth of the previously described successive oscillatory field technique[1] and of the atomic beam experiments with stored atoms.[2–4] The hydrogen maser also incorporates many of the features of beam maser developed by Townes and his associates.[5,6] The experiments are also related to the buffer gas experiments of Dicke[7,8] and others although no buffer gas is used in the hydrogen maser. A preliminary report on the hydrogen maser has been published[4] but no detailed analysis of its characteristics has been published previously.

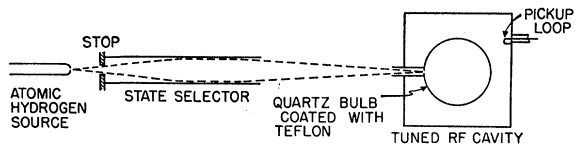

FIG. 1. Schematic diagram of the hydrogen maser.

The hydrogen maser consists of the apparatus shown schematically in Fig. 1. Atomic hydrogen from a radiofrequency discharge in the source passes through the inhomogeneous state-selecting magnetic field from a 6-pole permanent magnet. This field focuses atoms in the $[F=1, m=0]$ and $[F=1, m=1]$ states onto an aperture in a Teflon coated quartz bulb. The bulb is located in the center of a cylindrical radiofrequency cavity, operating in the TE_{011} mode, which is tuned to the $[F=1, m=0] \rightarrow [F=0, m=0]$ hyperfine transition frequency at approximately 1420.405 Mc/sec. The atoms make random collisions with the Teflon coated bulb wall and eventually leave the bulb through the entrance aperture. Due to their small interaction with the Teflon surface the atoms are not seriously perturbed even though they are retained in the bulb for more than a second and undergo up to 10^5 collisions with the wall during the storage time. Under these conditions the resonance line is so sharp that self-excited maser oscillations at the hyperfine frequency can take place.

The hydrogen maser has advantages in all of the desirable features listed above: (a) since the transition time is longer than one second the resonance line is narrow; (b) the hydrogen atom spends most of its time

* Work supported by the National Science Foundation and the Joint Program of the Office of Naval Research and the Atomic Energy Commission.

[1] N. F. Ramsey, Rev. Sci. Instr. **28**, 57 (1957); N. F. Ramsey, *Molecular Beams* (Oxford University Press, New York, 1956), p. 124.
[2] D. Kleppner, N. F. Ramsey, and P. Fjelstad, Phys. Rev. Letters, **I**, 232 (1958).
[3] H. M. Goldenberg, D. Kleppner, and N. F. Ramsey, Phys. Rev. **123**, 530 (1961).
[4] H. M. Goldenberg, D. Kleppner, and N. F. Ramsey, Phys. Rev. Letters **5**, 361 (1960).
[5] J. P. Gordon, H. J. Zeiger, and C. H. Townes, Phys. Rev. **95**, 282 (1954); N. G. Basov and A. M. Prokhorov, J. Exptl. Theoret. Phys. (U.S.S.R.) **27**, 431 (1954).
[6] K. Shimoda, T. C. Wang, and C. H. Townes, Phys. Rev. **102**, 1308 (1956).
[7] R. H. Dicke, Phys. Rev. **89**, 472 (1953).
[8] J. P. Wittke and R. H. Dicke, Phys. Rev. **103**, 620 (1956).

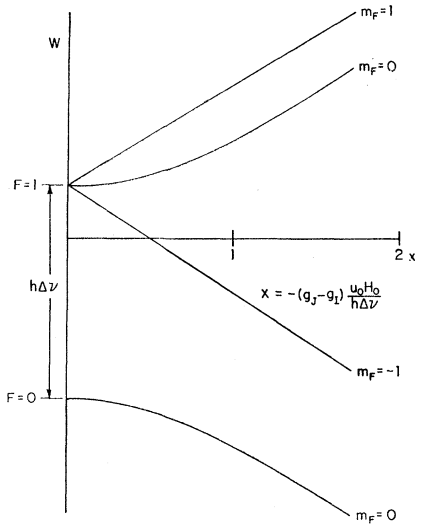

FIG. 2. Energy levels of the $^2S_{\frac{1}{2}}$ state of hydrogen.

in free space where it has a simple unperturbed hyperfine spectrum and the effects of wall collisions are small due to the low electric polarizability; (c) the effect of the first-order Doppler shift is greatly reduced by the fact that the velocity of the atom in the bulb, when suitably averaged, is close to zero; and (d) the ability of the device to operate as a self-excited maser oscillator provides the advantages of low noise amplification which characterize masers.

In the present paper the detailed theory and characteristics of the hydrogen maser are presented. Some preliminary experimental results have already been published[4] and details of the apparatus[9] and further results will be published subsequently.

II. STATIONARY OSCILLATION

Several authors have analyzed the behaviour of a two-level microwave beam maser.[6,10,11] The treatment of the ammonia maser by Shimoda, Wang, and Townes[6] (SWT) is the most comprehensive and the discussion of this section follows their analysis where possible. The chief differences are: (a) the transition of interest here is magnetic dipole, rather than electric dipole; (b) the lifetime of the atoms is described by an exponential distribution function instead of being constant; and (c) effects of confinement of the radiating atoms by the storage bulb must now be considered.

A. Preliminary Discussion

The ground state of hydrogen in a magnetic field $\mathbf{H}_0$ is described by the Hamiltonian

$$\mathcal{H}=ha\mathbf{I}\cdot\mathbf{J}-g_J\mu_0\mathbf{J}\cdot\mathbf{H}_0-g_I\mu_0\mathbf{I}\cdot\mathbf{H}_0. \tag{1}$$

The energy levels are illustrated in Fig. 2. In the presence of an oscillating magnetic field which lies in the direction of the static field so that $\mathbf{H}=(H_0+H_z\cos\omega t)\mathbf{k}$, the $(F=1, m_F=0)$ and $(F=0, m_F=0)$ states are connected by the following matrix element:

$$\begin{aligned}(0,0|\mathcal{H}|1,0)=(1,0|\mathcal{H}|0,0)&=(g_J-g_I)\tfrac{1}{2}\mu_0 H_z\cos\omega t\\ &\approx-\mu_0 H_z\cos\omega t.\end{aligned} \tag{2}$$

The wave function may be written

$$\psi=a_1\psi(0,0)+a_2\psi(1,0). \tag{3}$$

If at time $t=0$ the atom is in the $(F=1, m_F=0)$ state, then it can be shown[12] that at time t later

$$\begin{aligned}a_1(t)&=-\exp\left[\frac{i}{2}(\omega-\omega_0)t\right]\frac{x}{[(\omega-\omega_0)^2+x^2]^{\frac{1}{2}}}\\ &\quad\times\sin\{\tfrac{1}{2}[(\omega-\omega_0)^2+x^2]^{\frac{1}{2}}t\},\\ a_2(t)&=\exp\left[\frac{-i}{2}(\omega-\omega_0)t\right]\left[\frac{-(\omega-\omega_0)}{[(\omega-\omega_0)^2+x^2]^{\frac{1}{2}}}\right.\\ &\quad\times\sin\{\tfrac{1}{2}[(\omega-\omega_0)^2+x^2]^{\frac{1}{2}}t\}\\ &\quad\left.+i\cos\{\tfrac{1}{2}[(\omega-\omega_0)^2+x^2]^{\frac{1}{2}}t\}\right],\end{aligned} \tag{4}$$

where $x=-\mu_0 H_z/\hbar$, $\omega_0=[W(1,0)-W(0,0)]/\hbar$.

The average power radiated by a beam of I atoms per second initially in the (1,0) state is

$$\Delta P=Ih\nu\langle|a_1|^2\rangle_{\rm av}, \tag{5}$$

(SWT use the symbol "n" instead of "I.") Here the average is over time spent in the cavity by the atoms. It will be shown below that the probability that an atom ceases to radiate by leaving the bulb or by having its radiation state relaxed is described by a simple exponential distribution function,

$$f(t)=\gamma\exp(-\gamma t), \tag{6}$$

in which case Eqs. (4) and (5) yield, after the indicated averaging,

$$\Delta P=\tfrac{1}{2}Ih\nu\frac{x^2}{\gamma^2+x^2+(\omega-\omega_0)^2}. \tag{7}$$

In the hydrogen maser the atoms, on the average, make many traversals of the storage bulb before leaving the cavity. As will be shown in Sec. IV-E, if H_z is not

[9] D. Kleppner, H. M. Goldenberg, and N. F. Ramsey, *Applied Optics* **1**, 55 (1962).

[10] H. M. Goldenberg, thesis, Harvard University, 1960 (unpublished).

[11] J. P. Gordon, H. J. Zeiger, and C. H. Townes, Phys. Rev. **99**, 1264 (1955); R. P. Feynman, F. L. Vernon, and R. W. Hellwarth, J. Appl. Phys. **28**, 49 (1957); W. E. Lamb and J. C. Helmer, Stanford University Microwave Laboratory Technical Report No. ML-311 (unpublished).

[12] N. F. Ramsey, *Molecular Beams* (Oxford University Press, New York, 1956), p. 119.

uniform throughout the storage bulb, we may replace x^2 by

$$\langle x\rangle^2=(\mu_0/\hbar)^2\langle H_z\rangle_b^2, \tag{8}$$

where $\langle H_z\rangle_b$ is averaged over the volume of the storage bulb. The energy stored in the resonant cavity is

$$W=\frac{1}{8\pi}\int_V H^2dV. \tag{9}$$

(H is the peak value of the oscillating magnetic field and the average is over the volume of the resonant cavity.) $\langle H_z\rangle_b^2$ is related to the stored energy by $\langle H_z\rangle_b^2=(8\pi W/V)\eta$ where $\eta=\langle H_z\rangle_b^2/\langle H^2\rangle_V$. The value of η is plotted in Fig. 3, as a function of a/l, the ratio of storage bulb radius to cavity diameter, for a TE_{011} cavity with length and diameter equal. Combining the above expression with Eq. (7) yields

$$\Delta P=\tfrac{1}{2}Ih\nu\frac{\theta^2}{1+\theta^2+\delta^2}, \tag{10}$$

$$\theta^2=\langle x^2\rangle/\gamma^2=W/W_c,\quad W_c=(h/\mu_0)^2V\gamma^2/8\pi\eta,\qquad \delta=(\omega-\omega_0)/\gamma. \tag{11}$$

The resonance curve is Lorentzian. The full resonance width at half-height, assuming $\theta^2\ll 1$, is

$$\Delta\omega_r=2\gamma. \tag{12}$$

B. Threshold Flux

For oscillation to occur, the power delivered to the cavity by the beam must equal the power dissipated in the cavity. The condition for this is

$$W=\frac{Q\Delta P}{\omega}=\frac{1}{2}\frac{Q}{\omega}Ih\nu\frac{\theta^2}{1+\theta^2}. \tag{13}$$

Near the threshold of oscillation $\theta\ll 1$, and from Eqs. (11) and (13), the minimum flux necessary for oscillation is

$$I_{\rm th}=4\pi W_c/Qh=hV\gamma^2/8\pi^2\mu_0^2Q\eta. \tag{14}$$

As an example, if $V=10^4$ cm^3, $\gamma=0.3$ sec^{-1}, $Q=3\times10^4$, $\eta=3$, we have $I_{\rm th}=10^{12}$ pps. With an incident beam $I>I_{\rm th}$, the level of stored energy is given by

$$W/W_c=\theta^2=(I/I_{\rm th})-1. \tag{15}$$

If the output coupling is represented by Q_1, then the output power is, using Eqs. (14) and (11),

$$P_0=\frac{\omega W_c}{Q_1}\left(\frac{I}{I_{\rm th}}-1\right). \tag{16}$$

C. Effect of the Cavity Tuning on the Oscillator Frequency

In order to analyze the effect of cavity tuning and noise in the maser, the oscillating dipole moment due to the stored atoms is calculated in the presence of an assumed oscillatory magnetic field. The electromagnetic field generated by the oscillating magnetization is then calculated, and the assumed field is made consistent with the field produced. The effects of thermal noise are ignored in this section but will be considered below.

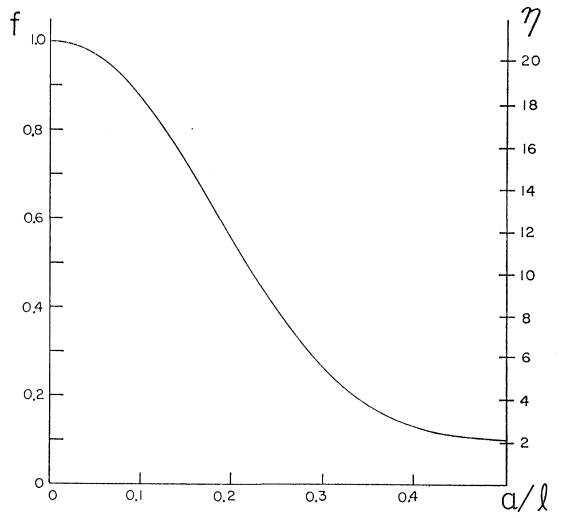

FIG. 3. The functions $\eta=\langle H_z\rangle^2/b\langle H^2\rangle_V$ and $f=\langle H_z\rangle_b^2/H_z^2(\max)=0.047\eta$ for a storage bulb of radius a in a TE_{011} cavity with diameter and length equal to l.

The dipole moment operator is

$$\boldsymbol{\mu}(\text{op})=g_J\mu_0\mathbf{J}+g_I\mu_0\mathbf{I}. \tag{17}$$

The oscillating dipole moment of an atom in the cavity at any time is

$$\mu=\int\psi^*\boldsymbol{\mu}(\text{op})\psi d\tau=(a_2^*a_1+a_1^*a_2)\mu_0, \tag{18}$$

where g_J has been approximated by 2 and g_I by zero. (Vector notation has been omitted since the direction of the oscillating moment is parallel to the driving field, which is along the z axis.) When the perturbing field is $H_z\cos\omega t$, the dipole moment of an atom at time t which entered the field at time t_0 is, from Eqs. (4) and (18),

$$\mu(t-t_0)=\mu_0e^{i\omega t}\frac{x}{[(\omega-\omega_0)^2+x^2]^{\frac{1}{2}}}\times\left[\frac{i}{2}\sin\{[(\omega-\omega_0)^2+x^2]^{\frac{1}{2}}(t-t_0)\}+\frac{(\omega-\omega_0)}{[(\omega-\omega_0)^2+x^2]^{\frac{1}{2}}}\sin^2\left\{[(\omega-\omega_0)^2+x^2]^{\frac{1}{2}}\frac{(t-t_0)}{2}\right\}\right]$$
$$+\text{complex conj.}=\mu^\dagger e^{i\omega t}+\mu^{\dagger *}e^{-i\omega t}. \tag{19}$$

The oscillating magnetization $M(\mathbf{r})$, produced by the

atoms in the cavity, is given by

$$M(\mathbf{r})=\frac{I}{\gamma V_b}\bar{\mu}(\mathbf{r})=\frac{I}{\gamma V_b}[\bar{\mu}^{\dagger}e^{i\omega t}+\bar{\mu}^{\dagger *}e^{-i\omega t}]. \quad (20)$$

The bar denotes an average over $(t-t_0)$, the time spent in the cavity. The probability that an atom has spent a time $(t-t_0)$ in the cavity is $\gamma\exp[-\gamma(t-t_0)]$. When the average is carried out, Eqs. (19) and (20) yield, assuming $\omega-\omega_0\ll x$.

$$M(\mathbf{r})=\frac{I\mu_0}{2\gamma V_b}\frac{x[\lambda+i\gamma]}{\gamma^2+x^2+(\omega-\omega_0)^2}e^{i\omega t}+\text{c.c.} \quad (21)$$

The magnetic field H generated by the oscillating magnetization can be calculated in the following fashion: It is assumed that the magnetization is so small that it does not seriously perturb the normal mode of the cavity, or the distribution of field in that mode $\mathbf{H}_n$. In this case the quality factor of the cavity containing the oscillating magnetization Q_m can be calculated from a result given by Slater[13] for a cavity containing a microwave current.

$$\frac{1}{Q_m}-2i\frac{\omega-\omega_c}{\omega_c}=\frac{1}{Q}+4\pi i\frac{\int\mathbf{M}^{\dagger}(\mathbf{r})\cdot\mathbf{H}_n^{\dagger *}(\mathbf{r})dV}{\int\mathbf{H}^{\dagger}(\mathbf{r})\cdot\mathbf{H}_n^{\dagger *}(\mathbf{r})dV}. \quad (22)$$

Here $\omega_c/2\pi$ is the resonant frequency and Q is the loaded quality factor of the cavity without stored atoms, while the frequency of oscillation is $\omega/2\pi$. Both the field and magnetization are expressed here in complex vector notation: $H\cos\omega t=\frac{1}{2}(\mathrm{H}e^{i\omega t}+\mathrm{H}e^{-i\omega t})=H^{\dagger}e^{i\omega t}+H^{\dagger *}e^{-i\omega t}$, and $\mathbf{M}=M^{\dagger}e^{i\omega t}+M^{\dagger *}e^{-i\omega t}$.

After some manipulation Eq. (22) can be rewritten, with the aid of Eq. (21),

$$\frac{1}{Q_m}-2i\frac{\omega-\omega_c}{\omega_c}=\frac{1}{Q}+i\frac{8\pi^2\mu_0^2 I\eta}{h\gamma V}\left[\frac{\lambda+i\gamma}{\gamma^2+x^2+(\omega-\omega_c)^2}\right]. \quad (23)$$

For oscillation to occur $Q_m=\infty$, and Eq. (23) becomes, using Eq. (14),

$$1+2i\frac{(\omega-\omega_c)}{\omega_c}Q=\frac{I\gamma}{I_{\mathrm{th}}}\left[\frac{\gamma-i(\omega-\omega_0)}{\gamma^2+x^2+(\omega-\omega_0)^2}\right]. \quad (24)$$

If $\omega\approx\omega_0$, and $\omega-\omega_0\ll x$, the real part of Eq. (24) gives Eq. (15), while the imaginary part can be written

$$\omega-\omega_0=2\left(\frac{\omega_c-\omega_0}{\omega_0}\right)Q\gamma. \quad (25)$$

If we define the quality factor of the resonance line by

$$Q_l=\omega_0/\Delta\omega_r=\omega_0/(2\gamma). \quad (26)$$

[13] J. C. Slater, Revs. Modern Phys. **18**, 441 (1946).

Equation (25) becomes

$$\frac{\omega-\omega_0}{\omega_0}=\frac{(\omega_c-\omega_0)}{\omega_0}\frac{Q}{Q_l}. \quad (27)$$

This is a familiar result. In the case of the conventional beam maser, the expression on the right is multiplied by a slowly varying function of the power radiated. When the lifetime of the atom is described by an exponential distribution function, however, cavity pulling is independent of the power level.

D. The Effect of Thermal Noise on the Oscillation

In order to calculate accurately the effect of thermal noise on the maser it is necessary to take into account the amplification of the noise by the maser itself. This is done by a perturbation method in which the thermal noise field in the cavity $H_n(t)$ is assumed to be small compared to the field H_0 produced by coherent radiation of the atoms. Details of this procedure are discussed in SWT, and only an outline of the calculation is given here.

The oscillating field in the cavity is assumed to be of the form

$$H_z=H_{z0}\cos\omega t+H_n(t). \quad (28)$$

Let

$$x=H_{z0}\mu_0/\hbar, \quad x_n(t)=2H_n(t)\mu_0/\hbar. \quad (29)$$

The quantity x_n may be written

$$x_n(t)=2x_n'\cos\omega t-2x_n''\sin\omega t, \quad (30)$$

where x_n' and x_n'' are functions of time defined by the equation. Equation (28) becomes, assuming x_n' and x_n'' are much less than x,

$$H_z=\hbar\mu_0^{-1}(x+x_n')\cos(\omega t+x_n''/x), \quad (31)$$

which shows that x_n' represents amplitude modulation and x_n'' represents phase modulation.

The effect of the noise is to induce a fluctuating oscillating dipole moment. The total oscillating moment can be written

$$\mu=\mu_s^{\dagger}e^{i\omega t}+\mu_n^{\dagger}(t)+\text{complex conjugate}. \quad (32)$$

The first term represents the contribution of the atoms with no noise present, and the second term represents the contribution due to the noise.

It is shown in SWT that

$$\mu_s^{\dagger}=\tfrac{1}{2}i\mu_0\sin xt, \quad (33)$$

$$\mu_n^{\dagger}(t)=-\tfrac{1}{2}\mu_0 e^{i\omega t}\left[\int_{t_0}^{t}x_n''(t')\cos\{x(t'-t_0)\}dt'-i\cos\{x(t'-t_0)\}\int_{t_0}^{t}x_n'(t')dt'\right]. \quad (34)$$

The field which would be present in the cavity due to noise with no atoms present may be written

$$h_0(t)=h_n^{\dagger}e^{i\omega t}+h_n^{\dagger *}e^{-i\omega t}, \tag{35}$$

$$h_n^{\dagger}=2\hbar^{-1}(\xi_n'(t)+i\xi_n''(t))=2\hbar^{-1}\xi_n^{\dagger}(t). \tag{36}$$

$\xi_n'(t)$ and $\xi_n''(t)$ are derived from the spectral density in the cavity in the absence of the beam. In the following steps x_n' and x_n'' are found in terms of ξ_n' and ξ_n'', respectively, thereby giving the actual values for amplitude and frequency modulation in the oscillating maser.

For present purposes we need an equation similar to Eq. (24) but in which the dependence on the oscillating field is made explicit. This is obtained from Eq. (22) by using the value of $M(r)$ given by Eq. (20), assuming $Q_m=0$ and $Q(\omega-\omega_e)/\omega_c\ll 1$. If we solve the resultant equation for the field, we obtain

$$H_z^{\dagger}=-i\frac{4\pi Q\eta I}{V}\int_{-\infty}^{t}e^{-\gamma(t-t_0)}\mu^{\dagger}(t-t_0)dt_0+h_n^{\dagger}. \tag{37}$$

The first term on the right-hand side represents the field due to the oscillating magnetization, while the second term represents the thermal noise present with no magnetization. Using Eqs. (28), (33), (34), and (36), one obtains

$$\frac{x}{2}+\frac{x_n^{\dagger}}{2}-\frac{\xi_n^{\dagger}}{2}=\frac{4\pi^2IQ\eta u_0^2}{Vh}\Big[\int_{-\infty}^{t}e^{-\gamma(t-t_0)}\sin(x(t-t_0))dt_0$$
$$+i\int_{-\infty}^{t}e^{-\gamma(t-t_0)}\Big\{\int_{t_0}^{t}x_n''(t')\cos x(t'-t_0)dt'$$
$$-i\cos(x(t-t_0))\int_{t_0}^{t}x_n'dt'\Big\}dt_0\Big]. \tag{38}$$

The first integral yields the same result as found in Sec. II-B. The other terms represent the effect of noise and can be written

$$\frac{x_n^{\dagger}}{2}-\frac{\zeta_n^{\dagger}}{2}=(1+\theta^2)\gamma^2\int_{-\infty}^{t}e^{-\gamma(t-t_0)}\Big\{\cos(x(t-t_0))$$
$$\times\int_{t_0}^{t}x_n'(t')dt'+i\int_{t_0}^{t}\cos(x(t-t_0))x_n''(t')dt'\Big\}dt_0, \tag{39}$$

where we have made use of the identity

$$8\pi^2QI\eta u_0^2/Vh=I\gamma^2/I_{\text{th}}=(1+\theta^2)\gamma^2.$$

The real part of Eq. (39) can be solved for the case of noise components which lie within the resonance linewidth. With this restriction, $x_n'(t)$ may be considered constant, and the result is

$$2x_n'=\xi_n'(1+\theta^2)/\theta^2. \tag{40}$$

This result illustrates how the nonlinear properties of the maser oscillator tend to limit amplitude fluctuations, a familiar property of oscillators. As the oscillation level increases, the fractional amplitude fluctuation is suppressed. The fractional amplitude modulation, $x_n'/x=\xi_n'(1+\theta^2)/(2\gamma\theta^3)$, approaches zero with increasing radiated power.

In order to find the relation between x_n'' and ξ_n'' the time dependence of x_n'' must not be neglected. The reason for this that x_n'' represents a phase fluctuation which approaches infinity as time increases. The quantity of physical interest is the frequency fluctuation, and to determine this it is necessary to know how the phase x_n''/x increases in time. To do this we consider the spectral densities of ξ_n'' and x_n''. If df represents a frequency bandwidth differing from the oscillator frequency by f, we may write

$$\xi_n''(t)=\int_0^{\infty}\xi_n''(f)\cos(2\pi ft+\delta)df, \tag{41}$$

$$x_n''(t)=\int_0^{\infty}x_n''(f)\cos(2\pi ft+\delta')df, \tag{42}$$

where δ and δ' are phase angles, to be determined. With these substitutions, the imaginary part of Eq. (39) becomes

$$x_n''(f)\cos(2\pi ft+\delta')-\xi_n''(f)\cos(2\pi ft+\delta)$$
$$=(1+\theta^2)\gamma^2\int_{-\infty}^{t}e^{-\gamma(t-t_0)}\int_{t_0}^{t}x_n''(f)\cos(2\pi ft'+\delta)$$
$$\times\cos(x(t'-t_0)dt'dt_0. \tag{43}$$

The result of Eq. (43) is

$$\delta-\delta'=\pi/2 \tag{44}$$

and

$$x_n''(f)=\xi_n''(f)\frac{\gamma}{2\pi f}.$$

It is shown in SWT that

$$\frac{\langle\xi_n^2(f)\rangle_{\text{av}}}{x^2}=\frac{kTdf}{\omega_0W/Q},$$

so that

$$\frac{x_n''^2}{x^2}=\frac{QkT}{\omega_0W}\left(\frac{\gamma}{2\pi}\right)^2\int_{f_{\min}}^{f_{\max}}\frac{df}{f^2}, \tag{45}$$

($\langle\langle\ \rangle$ here represents the time average.)

Both $f_{\max}$ and $f_{\min}$ must be less than the linewidth in order for the approximation in $\mu^{\dagger}(t)$ to be valid. The lower limit is determined by the observation time. If the phase is observed for time t, then the smallest frequency fluctuation observable is $f_{\min}\cong 1/(2t)$.

Assuming that $f_{\max}\gg f_{\min}$, i.e., that the observation time is large compared to $2/\Delta\omega_r$, Eq. (45) becomes

$$\langle x''^2\rangle/x^2=QkT\gamma^2t/(2\pi^2\omega_0W). \tag{46}$$

The fractional rms frequency fluctuation is therefore

$$\frac{\langle\Delta\omega^2\rangle^{\frac{1}{2}}}{\omega_0}=\frac{\langle x'^2\rangle^{\frac{1}{2}}}{xt\omega_0}=\frac{\Delta\omega_r}{2\sqrt{2}\pi\omega_0}\left(\frac{QkT}{\omega_0 Wt}\right)^{\frac{1}{2}}$$

$$=\frac{0.113}{Q_l}\left(\frac{QkT}{\omega_0 W_c t}\right)^{\frac{1}{2}}\frac{1}{\theta}=\frac{0.113}{Q_l}\left(\frac{kT}{Pt}\right)^{\frac{1}{2}}. \quad (47)$$

In the last expression, P represents the power delivered by the beam to the cavity. For example, if $Q_l=2\times10^9$, $P=4\times10^{-5}$ erg/sec, $t=1$ sec, $\langle\Delta\omega^2\rangle^{\frac{1}{2}}/\omega_0=1.5\times10^{-15}$.

III. TRANSIENT OPERATION

The radiation lifetime of atoms in the cavity γ^{-1} can be found in principle from the response of the maser to an applied signal when it is operated below oscillation threshold as a spectrometer. This method involves sweeping the frequency of a local signal generator across the resonance curve and detecting the power emitted by stimulated emission. In practice it presents several difficulties. The most serious of these is the necessity for controlling the power level of the signal generator in order to avoid power broadening of the resonance line. Spurious pickup in the detecting system can be a source of difficulty with the low power levels involved. Achieving the necessary frequency stability in the signal generator can be another serious source of difficulty. All of these problems are avoided by a transient technique which allows direct measurement of the radiation lifetime.

The atoms can be put in a radiative state by a short pulse of power at the resonance frequency applied to the cavity when the density of atoms is insufficient to cause oscillation. A signal at the resonance frequency is then generated in the cavity by the atoms and, as is shown below, if the system is sufficiently below the threshold of oscillation, the amplitude of the signal decreases with decay constant characterizing the lifetime. The effect is similar in principle to free precession in NMR. Since the transition of interest is a hyperfine transition, however, it is not correct to picture it in terms of a simple magnetic moment which undergoes a 90° pulse. Furthermore, since the radiation level is determined by stimulated emission, the term "free precession" is really a misnomer. For these reasons, the dynamical behavior of the system will be described in some detail.

It is assumed that the beam flux is well below the level necessary for oscillation. A pulse of rf is applied for a time $\tau\ll\gamma^{-1}$. The frequency ω_p is such that $|\omega_p-\omega_0|<x_1$, where the amplitude of the pulse H_p is related to x_1 by $x_1=\mu_0 H_p/\hbar$. At the end of the pulse the amplitude of the lower energy state is, from Eqs. (1) and (4),

$$a_1=\sin(\tfrac{1}{2}x_1\tau).$$

At a time t later,

$$a_1(t)=\sin[\tfrac{1}{2}(x_1\tau+xt)].$$

The rate at which an atom radiates energy is

$$\Delta P=h\nu\frac{d}{dt}(a_1(t)^2)=\tfrac{1}{2}h\nu x\sin(x_1\tau+xt). \quad (48)$$

(In this last step it must be remembered that if x is a slowly carrying function of time then xt is to be interpreted as $\int_0^t x dt$.) If the energy level in the cavity is so low that $xt\ll1$ for all time less than γ^{-1}, then the atom radiates at a maximum rate when $x_1\tau=\pi/2$. Since $\tau\ll\gamma^{-1}$, the total number of atoms initially in this state is approximately $I\gamma^{-1}$, and at time t the number of radiating atoms is $I\gamma^{-1}e^{-\gamma t}$. The power radiated at time t is, therefore,

$$\Delta P=\tfrac{1}{2}Ih\nu\gamma^{-1}xe^{-\gamma t}. \quad (49)$$

The energy in the cavity obeys the following equation

$$dW/dt=\Delta P-\omega W/Q. \quad (50)$$

Using Eq. (11), this leads to

$$\frac{d}{dt}\theta^2=\frac{Ih\nu\theta}{2W_c}e^{-\gamma t}-\frac{\omega\theta^2}{Q}. \quad (51)$$

The solution to this equation, assuming $\omega/Q\gg2\gamma$, is

$$\theta=\frac{\pi}{2\gamma\tau}e^{-\omega/(2Q)t}+\frac{IhQ}{4\pi W_c}e^{-\gamma t}. \quad (52)$$

The first term, which corresponds to decay of the stimulating pulse due to losses in the cavity, quickly becomes negligible compared to the second. After this time the field intensity decreases with the decay constant γ. The energy in the cavity decreases at twice this rate. If the maser is monitored with a linear detector, however, the observed signal is proportional to the field intensity, and therefore yields a direct measure of the lifetime of the atoms.

Near threshold, the above analysis does not hold due to the nonuniform fashion in which the atoms radiate when $xt\approx1$, and due to the necessity of taking into account the effect of atoms which enter the cavity after the pulse is over. The behavior of the system in this region has been analyzed,[10,14] but the results are not experimentally as useful due to the complexity of interpretation in the present case.

IV. RELAXATION PROCESSES

A variety of processes can limit the radiative lifetime of an atom in the storage bulb. Most of the processes are random and lead to time independent relaxation rates, so that the total relaxation rate is the sum of the rates for each process. Because of this it is possible to analyze the relaxation processes separately, with the

[14] R. H. Dicke, Phys. Rev. **93**, 99 (1953); R. H. Dicke and R. H. Romer, Rev. Sci. Instr. **26**, 915 (1955); S. Bloom, J. Appl. Phys. **27**, 785 (1956).

understanding that the individual rates are to be added to obtain the tota' rate.

In the case of nuclear magnetic resonance, the dynamical equations of the magnetization are often described by the Bloch equations in terms of the relaxation times T_1 and T_2, the time constants which describe the return of magnetization in a given direction to its equilibrium value, and the decay of the oscillating dipole moment, respectively. These are not used in the present analysis because the Bloch equations do not apply due to the presence of hyperfine structure. It is important to remember, however, that a given perturbation frequently causes relaxation by both changing the magnetization along the axis of quantization and by causing loss of coherence between the oscillating moment and the rf field, and that these two rates may be considerably different. To emphasize this, the subscripts 1 and 2 will be used to identify decay rates due to each of these processes, respectively.

A. Escape from the Bulb

The escape rate of atoms from the bulb γ_0 is found by equating the incident beam flux I with the emergent flux, $N\bar{v}A_e/4K$, where N is the density, $\bar{v}$ is the mean velocity, A_e is the total escape area, and K is a numerical factor depending on the geometry of the first aperture. For a thin hole, $K=1$. If the volume of the storage bulb is V_b, then $N=I/(\gamma_0 V_b)$, and

$$\gamma_0=\bar{v}A_e/(4KV_b). \tag{53}$$

As an example, for hydrogen at room temperature, $\bar{v}=3\times10^5$ cm/sec, and for a spherical bulb 16 cm in diameter with a thin exit aperture 2 mm in diameter, $\gamma_0=1$ sec^{-1}.

B. Effect of Wall Collisions

Wall collisions fall conveniently into two categories: adiabatic and nonadiabatic. During an adiabatic collision no transitions of the atom between its states are induced but a small change in the spacing of the energy levels usually occurs. This eventually leads to a loss of coherence with the applied rf field due to randomness of the perturbations. In a nonadiabatic collision, the atom is effectively lost as far as further contributions to the radiation field are concerned due to a transition to some other state or to a chemical reaction with the surface. In this case, relaxation occurs during a single collision. The mean number of collisions an atom undergoes is then inversely proportional to the probability that a single collision is nonadiabatic.

1. Adiabatic Collisions

A convenient parameter in describing an adiabatic collision is the phase shift per collision

$$\varphi=\int\frac{\delta W(1,0)-\delta W(0,0)}{\hbar}dt. \tag{54}$$

The integration is over the time of one collision, and δW is the difference in energy of a given state between the free space value and the value when surface forces are present. It is shown in reference 3 that the atom loses coherence after a number of collisions

$$n\approx 2/\varphi^2. \tag{55}$$

This result was derived for a somewhat different situation from the present. In particular, it was assumed that there is no rf field present and that the adsorbtion energy is large compared with kT, so that the adsorbtion time is described by an exponential distribution function. Nevertheless, since the result is fundamentally due to the random nature of the perturbation, it is quite general and can be applied to the present case. (For example, it can be shown that the dispersion in φ is changed only slightly when the adsorbtion energy becomes less than kT, due to the relatively high dispersion in velocity and direction of the colliding atom.) If the collision rate is $\bar{v}/l$ then from Eq. (55) it follows that the relaxation rate is given by

$$\gamma_s=\tfrac{1}{2}(\bar{v}/l)\varphi^2. \tag{56}$$

This type of relaxation process does not strictly lead to a Lorentzian resonance line. However, in the case where this is not the dominating process the line is approximately Lorentzian and the decay rate is still a useful parameter for describing the linewidth. An example of a case where this leads to a non-Lorentzian line is given in reference 3.

The phase shift φ is related to the frequency shift, as discussed below. For the case of hydrocarbon-like surfaces an upper limit to φ is[10] $\varphi<10^{-4}$ rad/col, leading to a value of $\gamma_s<10^{-4}$ sec^{-1}.

2. Nonadiabatic Collisions: Chemical Reaction with the Surface

If there are no strong adsorbtion forces present, then physical adsorbtion does not by itself limit the radiative lifetime. Chemical reaction between the atom and the surface can occur, however, and this leads to a decay rate γ_s which is the probability per unit time that an atom undergoes such a reaction. This is found in the following manner: In order for a reaction to take place the incident atom must possess kinetic energy equal to E_a, the activation energy for that reaction. Departures of the atom from thermal equilibrium are usually negligible, so that the energy distribution may be found from a Maxwell-Boltzmann velocity distribution characterized by the temperature of the storage bulb. The probability that a particular collision leads to chemical reaction is obtained by finding the probability that the energy available for the reaction exceeds E_a. With the neglect of the difference between collisions of hydrogen with the same molecule when it is in the gas phase or on the surface, the following result for the rate r with

which the atoms hit the surface with an energy greater than E_a may be derived by well-known procedure[15]

$$r=(2\bar{v}/\pi^{\frac{1}{2}}l)\exp(-E_a/kT), \tag{57}$$

$\bar{v}$ is the rms velocity $(3kT/m)^{\frac{1}{2}}$, and l is the mean distance between collisions. For a sphere, l is two-thirds the diameter. The temperature T is that of the storage bulb. The reaction rate differs from r by the steric factor[16] P which is introduced because not every collision satisfying the energy requirement leads to a reaction. The relaxation rate is therefore

$$\gamma_r=(2\bar{v}P/\pi^{\frac{1}{2}}l)\exp(-E_a/kT). \tag{58}$$

Both E_a and P are difficult to estimate accurately for a surface collision. For reactions in the gas phase, P is usually taken to be 0.1, although it can be much smaller. Since a surface collision may involve interaction with several of the surface molecules, P is probably larger than for a similar collision in the gas phase. A particular example of a possible surface reaction is the case of surface combination which occurs when atomic hydrogen reacts with a methyl group which is part of a hydrocarbon surface. An example of this is $H+CH_3\rightarrow H_2+CH_2$ where it is understood that the methyl group is bonded to a larger molecule. To estimate the activation energy for this reaction, one may consider a similar reaction which has been observed in the gas phase, $H+C_2H_6\rightarrow H_2+C_2H_5$. The activation energy for this is 6.4 kcal/mole (0.27 ev),[17] with a steric factor of about 5×10^{-3}. The activation energy for reactions involving hydrogen recombining with other paraffin hydrocarbons does not vary markedly from this value with the size of the molecule, so that it is a reasonable value to use for the present case. When it is substituted into Eq. (58), and assuming $P=1$, the result for a 16-cm-diam bulb at room temperature is $\gamma=0.7$ sec^{-1}. This is in approximate agreement with experimental observations which will be described in a later paper. The activation energy for corresponding reactions with flurocarbon is considerably higher than for the hydrocarbons, and the decay rate with a Teflon surface has been found to be considerably smaller than possible with a hydrocarbon surface.

C. Effect of Magnetic Field Inhomogeneities

A nonuniform static magnetic field in the storage bulb can cause relaxation in two ways. The atoms experience a time-varying field by virtue of their motion through the bulb, and this can induce Zeeman transitions analogous to the Majorana transitions of atomic beams. In addition, since the resonance frequency is slightly field dependent, and because different atoms have different histories in the bulb, due to the random nature of their paths, there is eventually a loss of coherence of the oscillating moment. The relaxation rates due to these processes will be designated γ_{H1} and γ_{H2}, respectively.

1. Relaxation Rate γ_{H1}

The effect of the inhomogeneities on the Zeeman states ($F=1$, $m_F=1, 0, -1$) is most easily analyzed by neglecting the ($F=0$) state, and considering a spin 1 system in the presence of a random perturbation. Transitions are induced among the states at a rate W, and the decay rate for an atom from the state of interest, ($F=1$, $m=0$), is $\gamma_{H1}=W_{1,0}+W_{-1,0}$. The subscripts denote m_F. It should be noted that γ_{H1} does not correspond to T_1^{-1}, since the quantity of interest is the rate of decay of an atom from a given state, not the rate of decay of magnetization. In the latter case, for a spin $\frac{1}{2}$ particle, the rate is twice as great.

The transition rate between two states, α and β, due to a random perturbation $\mathcal{H}_1(t)=AF(t)$, where A is one operator and $F(t)$ is a random function, is[18]

$$W_{\alpha\beta}=\hbar^{-2}|(\alpha|A|\beta)|^2J(\omega_{\alpha\beta}), \tag{59}$$

$J(\omega_{\alpha\beta})$ is the spectral density of $\langle[F(t)]^2\rangle_{\rm av}$ and is given by the Fourier transform of the autocorrelation function of $F(t)$. The interaction Hamiltonian is

$$\mathcal{H}=-\gamma_F\hbar\mathbf{F}\cdot\mathbf{H}(t). \tag{60}$$

To a good approximation the components of the inhomogeneous magnetic field vary independently, so that $H(\mathbf{t})=H_x(t), H_y(t), H_z(t)$. When this is substituted in Eqs. (60) and (59) we have

$$W_{1,0}=W_{-1,0}=\tfrac{1}{2}\gamma_F{}^2J(\omega), \tag{61}$$

$$J(\omega)=\int_{-\infty}^{+\infty}[(H_x(t)+H_y(t)]\times[H_x(t+\tau)+H_y(t+\tau)]e^{-i\omega\tau}d\tau. \tag{62}$$

The cross products in the above equation vanish because $H_x(t)$ and $H_y(t)$ are independent and have zero average, so that $\langle H_x{}^2\rangle_{\rm av}=\langle H_y{}^2\rangle_{\rm av}=\frac{1}{2}\langle H_t{}^2\rangle_{\rm av}$. The autocorrelation function of H_t, the transverse field, is $g(\tau)=\langle H_t(\tau)H_t(t+\tau)\rangle$, and the result is

$$\gamma_{H1}=W_{1,0}+W_{-1,0}=\gamma_F{}^2\int_{-\infty}^{+\infty}g(\tau)e^{-i\omega\tau}d\tau. \tag{63}$$

The integral in this equation, the spectral density of $\langle H_t{}^2\rangle_{\rm av}$ at the transition frequency, is a complicated function of the storage bulb geometry, velocity distribution, and magnetic field. The mean time between collisions t_0 naturally presents itself as a sort of correlation time, since the motion of the atom is altered

[15] R. Fowler and E. A. Guggenheim, *Statistical Thermodynamics* (Cambridge University Press, London, 1956), Chap. XII.

[16] E. W. R. Steacie, *Atomic and Free Radical Reactions* (Reinhold Publishing Corporation, New York, 1954), p. 490.

[17] M. R. Berlie and D. J. LeRoy, Discussions Faraday Soc. **14**, 50 (1953).

[18] A. Abragam, *The Principles of Nuclear Magnetism* (Oxford University Press, London, 1961), p. 270.

violently and nearly randomly on each wall collision, and in spite of the complexity of $g(\tau)$ it is possible to obtain approximate expression for the spectral density in the cases when ω is either much less or much greater than t_0^{-1}.

In the limit of low magnetic fields $\omega=\gamma_F H_0 \ll t_0^{-1}$ and the wall collision occurs rapidly with respect to ω^{-1}. In this case the atoms experience a field which assumes a new value after every collision, and if the wall collisions occur perfectly randomly in time, then[19]

$$g(\tau)=\langle H_t^2\rangle_{\rm av} e^{-|\tau|/t_0}, \tag{64}$$

where the average of $\langle H_t^2\rangle_{\rm av}$ is over either time or space. In this limit, we find

$$\gamma_{H1}(\omega \ll t_0^{-1})=2\gamma_F^2\langle H_t^2\rangle_{\rm av} t_0. \tag{65}$$

This expression is not valid when $\omega \gtrsim t_0^{-1}$ for the following reason[20]: the assumption that the field changes discontinuously is not valid even in the low field case, although it introduces no appreciable error there since the relatively large intensity high-frequency components led to by this model have no effect when the resonance is at a low frequency. In the present case, however, the transitions are sensitive to the high-frequency components. Actually, the field is not discontinuous in time, since the atom does not alter position instantaneously, but its time derivative is discontinuous as long as the wall collision takes place in a time small compared to ω^{-1}. It can be shown that this causes the spectral density to fall off as ω^{-4}. Since the discontinuities in dH/dt occur at a surface collision, the spectral density is now sensitive only to the average field inhomogeneity at the surface, rather than the average throughout the bulb. Because of this it is necessary to assume a certain field configuration in order to estimate $J(\omega)$. The relaxation rate has been derived by Purcell[20] for the simplest type of symmetrical field inhomogeneity, where the inhomogeneous field is given in cylindrical coordinates by $H_\rho=2h\rho z/d^2$ $\cdot H_z=(h/a^2)(\rho^2-2z^2)$. The result is

$$\gamma_{H1}=\tfrac{1}{2}\gamma_F^2 h^2 \frac{t_0}{1+(\omega t_0/2)^4}. \tag{66}$$

As an example, in the low field region where $\omega t_0 \ll 1$, then the factor $(\omega t_0/2)^4$ may be neglected and using $\gamma_F=1.4\times10^6$ cps/oe, $t_0=3\times10^{-5}$ sec, the result is $\gamma_{H1}=3\times10^7 H_t^2$, so that for $H_t=10^{-4}$ oe, $\gamma_{H1}=0.3$ sec^{-1}.

This process leads to a non-Lorentzian line shape since it affects only the upper of the two resonance states. In the case where it is the dominating mechanism, the line shape does become Lorentzian, much as an ideal optical transition has a Lorentzian line shape even though the upper state has a very large decay rate and the lower state has a decay rate of zero. If there are several competing processes the situation is quite complicated, although it can be solved if the total decay rate for each of the states is known.[21]

2. *Relaxation Rate* γ_{H2}

The same comments regarding the line shape that were made in Sec. IV B(1) apply to phase decorrelation due to random motion through an inhomogeneous field. A simple method with which to obtain an estimate of γ_{H2} is to assume that the field has a separate value on either half of the storage bulb, $H_0\pm\Delta H/2$. Since field dependence of $(F=1, m_F=0)\rightarrow(F=0, m_F=0)$ is given by $\nu=\nu_0+\alpha H^2$, where $\alpha=2750$ cps/oe^2, the resonance frequencies on either side of the bulb then differ by $2\alpha H_0\Delta H$, assuming $\Delta H \ll H_0$. If the mean number of collisions an atom makes before leaving is n, then the mean time an atom spends in one half of the bulb, in excess of the other half, is $2n^{\frac{1}{2}}t_0$, and for coherence it is necessary to have $2n^{\frac{1}{2}}t_0(2\alpha H_0\Delta H)<1$. Therefore,

$$\gamma_{H2}=1/nt_0=t_0(16\alpha^2 H_0^2\Delta H^2). \tag{67}$$

If, for example, $H_0=10^{-2}$ oe, $\Delta H=10^{-3}$ oe parallel to H_0, then with $t_0=3\times10^{-5}$ sec, we have $\gamma_{H2}\cong10^{-6}$ sec^{-1}.

If the transitions of interest are $(F=1, m_F=\pm1)\rightarrow(F=0, m_F=0)$, the π transitions, then there is a first-order field dependence, $\nu=\nu_0\pm\beta H$, where $\beta=1.4\times10^6$ cps/oe, and it follows that

$$\gamma_{H1}(\pi)=4\beta^2\Delta H^2 t_0. \tag{68}$$

With the same field as above, $\gamma_{H1}(\pi)=240$ sec^{-1}. On the other hand, if the field varies due to inhomogeneities which are only perpendicular to the axis, then an inhomogeneity of 10^{-3} oe in the same field as above yields $\gamma_{H1}(\pi)=0.6$ sec^{-1}.

D. Spin Exchange Relaxation

At sufficiently high density of atomic hydrogen the dominating relaxation process is due to hydrogen-hydrogen collisions. The mechanism which leads to relaxation is chiefly spin exchange in which the electron spins of the colliding atoms exchange, leaving the atoms in hyperfine states different from the initial states. Wittke and Dicke[8] have analyzed this process, and their results have recently been confirmed by a detailed analysis of Mazo.[22] Measurements of the spin exchange cross section have been made in an EPR experiment by Hildebrandt, Booth, and Barth[23] and there is generally good agreement between theoretical and experimental results. The decay rate for spin exchange collisions $\gamma_{\rm se}$ is related to the number of hydrogen atoms per cm^3, N, by

$$\gamma_{\rm se}\cong5\times10^{-10}N \text{ sec}^{-1}. \tag{69}$$

[19] W. B. Davenport and W. L. Root, *An Introduction to the Theory of Random Signals and Noise* (McGraw-Hill Book Company, Inc., New York, 1958), p. 103.
[20] E. M. Purcell (private communication).
[21] P. Kusch and V. W. Hughes, *Handbuch der Physik*, XXXVII/1 (Springer-Verlag, Berlin, Germany, 1959), p. 7.
[22] R. M. Mazo, J. Chem. Phys. **34**, 169 (1961).
[23] A. F. Hildebrandt, F. B. Booth, and C. H. Barth, Jr., J. Chem. Phys. **31**, 273 (1959).

This expression, which is valid for EPR, should be slightly modified for the hydrogen maser since in the latter there is initially a nonequilibrium distribution of states. On the other hand, this introduces only a minor change in γ_{se}, and Eq. 69 is still correct for an approximate estimate.

E. First-Order Doppler Broadening

So far the effect of the Doppler shift on the shape of the resonance has been neglected. This might seem to be a poor approximation since the normal Doppler broadening of the hyperfine line for a free hydrogen atom moving with thermal velocities is over 10 kc/sec, more than 10^4 times the resonance width of interest in the hydrogen maser. Doppler broadening does not, in fact, contribute appreciably to the linewidth due to the confinement of the radiating atoms to a region of constant phase and only slightly varying field amplitude. The possibility of inhibiting Doppler broadening in paramagnetic resonance experiments by limiting the motion of radiating atoms was first pointed out by Dicke who has analyzed the case of a radiating atom moving diffusively through a region of varying phase.[7,8] The present situation differs in that the atoms are confined to a region of almost constant phase and varying field amplitude, and their motion is random within a confined volume, rather than diffusive. For these reasons, a brief analysis of the effect of the atoms' motion is given.

The situation can be visualized classically. The resonance curve for the system when the atoms are assumed to be at rest, Eq. (7), corresponds to the spectrum of an ensemble of damped harmonic oscillators. If the resonance is not appreciably saturated, i.e., if $x \ll \gamma$, then the transition probability, i.e., the intensity of the resonance, is proportional to the driving oscillating magnetic field intensity x^2, so that the field radiated by each member of the fictitious ensemble is proportional to the local driving field. In the most general case the amplitude and phase of the local driving field vary with position in space. This causes the atoms to experience random amplitude and phase fluctuations due to their random motion. In the present case the atoms are confined in a resonant cavity in a region of almost constant phase where the amplitude varies according to the field distribution of the mode. The quantity of interest is the spectral density of the radiated power $P(\omega)$. $P(\omega)$ is the Fourier transform of the autocorrelation function of $x(t)$, $G(\tau) = \langle x(t)x(t+\tau)\rangle$. If the oscillators were randomly distributed throughout the bulb, but were at rest, then $x(t+\tau)=x(t)\exp(-\gamma|\tau|)$. (The exponential term expresses the fact that we are dealing with damped oscillation.) In this case

$$G(\tau)=\langle x^2\rangle_b \exp(-\gamma|\tau|). \tag{70}$$

The average is over the volume of the storage bulb.

The atoms actually move rapidly, making on the average more than 10^4 collisions before leaving the bulb. All correlation between positions at successive times is lost after a few wall collisions, and for τ greater than the time for a few collisions $x(t+\tau)$ is independent of t, except for the damping factor. In this case, we have approximately

$$G(\tau)=\langle x\rangle_b^2 \exp(-\gamma|\tau|). \tag{71}$$

The effect of motion is to reduce the power radiated at the center of the resonance line. This may be seen by evaluating the ratio of the spectral density at the center of the resonance curve for the two cases

$$\frac{P(0)\text{ moving}}{P(0)\text{ rest}}=\frac{\langle x\rangle_b^2}{\langle x^2\rangle_b}=\frac{\langle H_z\rangle_b^2}{\langle H_z^2\rangle_b}. \tag{72}$$

The area lost from the center of the spectrum appears in a broad pedestal having the full Doppler width, $\Delta=\bar{v}/\lambda$. The spectrum is approximately

$$P(\omega)=\langle x\rangle^2\frac{1}{\gamma^2+\omega^2}+\frac{\Delta}{\gamma}(\langle x^2\rangle-\langle x\rangle^2)\frac{1}{\Delta^2+\omega^2}. \tag{73}$$

For a bulb located at a field maximum, $(\langle x^2\rangle-\langle x\rangle^2)/\langle x\rangle^2$ is typically $\frac{1}{10}(a/\lambda\!\!\!^{-})^2$, where it is assumed that the radius of the bulb, a, is small compared to $\lambda\!\!\!^{-}$, the cavity wavelength $\times(2\pi)^{-1}$. Since $\gamma\approx\bar{v}/na$, where n is the mean number of collisions, the ratio of the second to first terms of Eq. (73) for $\omega=0$ is approximately $a/(10n\lambda\!\!\!^{-})$. Consequently the contribution of the broadened term is negligible to the spectrum at resonance, and it has negligible effect on the half-width of the spectrum. On the other hand, the motion of the atoms does have a significant effect on the intensity of the resonance. The loss of intensity at $\omega=0$ is zero when the atoms are confined to a small volume at the region of maximum field, where $\langle x\rangle^2=\langle x^2\rangle=x_{\max}^2$. For larger regions, the intensity is reduced by the factor $f=\langle x\rangle^2/x^2(\max)$. This is related to the function η defined earlier by

$$f=\langle H^2\rangle_V\eta/H_z^2(\max). \tag{74}$$

In the case of a cylindrical cavity operating in the TE_{011} mode, $f=0.0474\eta$. Both f and η are plotted in Fig. 3 for a spherical bulb of radius a in such a cavity, with length l.

F. Second-Order Doppler Broadening

Although broadening of the resonance by the first-order Doppler shift has been shown to be negligible, the second-order Doppler shift must also be considered. It is shown in Sec. VI-C that the total fractional shift of frequency due to the second-order Doppler effect at room temperature is approximately 10^{-10}. The velocities of the atoms are described by a Maxwellian distribution, and if there were no thermalization with the walls the

resonance curve would be fractionally broadened by approximately the same amount as it is shifted. Thermalization does occur, however, and this reduces the effect. If the accommodation coefficient is p, and if the atoms make on the average n wall collisions, then the broadening effect is reduced by a factor approximately $(pn)^{\frac{1}{2}}$. Assuming $p=0.3$, $n=3\times10^4$, corresponding to a storage time of 1 sec, the broadening of the resonance line due to second-order Doppler shift is only about 1% of the resonance width, and therefore can be neglected.

G. Pressure Broadening

At easily obtainable pressures, collisions with inert atoms or molecules have negligible effect on the linewidth. Relaxation due to the presence of an impurity gas at elevated pressure has been observed. For instance, the relaxation rate due to O_2 has been found to be approximately

$$\gamma=2\times10^7 \text{ sec}^{-1}/\text{mm Hg}.$$

This effect is larger than can be accounted for by magnetic interaction and has not been fully interpreted as yet. It may be due to the formation of a short-lived excited molecule.

V. FREQUENCY SHIFTS IN THE MASER

Ideally the oscillation frequency of the maser is identical with the transition frequency between the levels of the atomic system as measured with atoms at rest in free space. The atoms are not free, though, since they interact with the surrounding electromagnetic system and, in the case of the present maser, with the walls of the storage bulb. In the following paragraphs some of the more important of the effects leading to a shift in frequency are discussed.

A. Wall Shift

The phase shift introduced in the wave function of an atom during a wall collision φ, defined in Eq. (54), causes a shift $\delta\omega$ in the resonance frequency given by

$$\delta\omega/\omega=\varphi/(\omega t_0), \tag{75}$$

where t_0 is the mean time between collisions. It is a difficult task to predict φ theoretically because of the uncertainty of the exact interaction potential and lack of knowledge of the microscopic wall structure. The experimental upper limit for φ for a surface treated with dimethyldichlorosilane is[10] $\varphi<10^{-4}$ rad, or, for a 16-cm-diam bulb, $\delta\omega/\omega<10^{-9}$. A lower limit to the expected shift with such a surface can be obtained from the following argument: The treated surface has very low adsorptive properties largely because it simulates a saturated hydrocarbon. The adsorption energy of atomic hydrogen on such surfaces is smaller than kT, and as a result the sticking time on the surface is comparable to the simple collision time with a free molecule. In a surface collision the impinging hydrogen atoms encounter methyl groups which are tightly bound to silicon atoms composing the underlying silica matrix. Such a collision should be similar but somewhat more severe than that with a single hydrogen molecule. The phase shift for the latter collision can be obtained from the measured value of the shift in the hyperfine frequency of hydrogen due to collisions with molecular hydrogen gas. This has been determined by Pipkin and his co-workers[24] and is -0.24 cps (mm Hg)$^{-1}$. Assuming an effective $H-H_2$ collision diameter of[25] 2.9×10^{-8} cm, the phase shift per collision is -3.9×10^{-3} rad/collision. This leads to a fractional shift in the frequency of the maser of $\delta\omega/\omega_0=-1.3\times10^{-13}$. The actual frequency shift with a saturated hydrocarbon surface should be higher than this value not only because the wall collision involves more than one perturbing molecule but because the small frequency shift in the molecular hydrogen buffer gas may be due to a partial cancellation of the dispersive attractive force effects by the effect of the exchange forces. The shift with a saturated flurocarbon surface, such as Teflon, may be smaller than the above value due to its relatively tight binding and small polarizability.

Since the wall shift is proportional to the collision rate, it can be determined by measuring the frequency of the maser as a function of the bulb size. This probably cannot be done with an accuracy of greater than 1% and the wall shift may therefore be the limiting factor in the absolute precision of the maser. Slow changes in the wall shift due to aging or contamination could cause long term fluctuations in the frequency. The answer to these problems can only be determined reliably by experiment.

B. First-Order Doppler Shift

The presence of running waves in the rf cavity can cause a shift in the resonance frequency due to the motion of the atoms. This occurs only if the atoms have a net effective translational velocity, as, for instance, if they enter one side of the bulb and relax before leaving through the entrance aperture. The situation is most easily described in terms of a running wave such as caused by the presence of a coupling loop placed asymmetrically in the cavity. (Effects of about the same size occur even if power is dissipated uniformly throughout the cavity walls due to generation of rf power within the storage bulb.) For the present, effects of saturation are neglected and an expression of the spectrum the atom experiences is derived by the same type of argument used in IV-E, to analyze the effect of Doppler broadening.

[24] L. W. Anderson, F. M. Pipkin, and J. C. Baird, Phys. Rev. Letters 4, 69 (1960).

[25] J. O. Hirschfelder, C. F. Curtiss, and R. B. Bird, *Molecular Theory of Gases and Liquids* (John Wiley & Sons, Inc., New York, 1954), p. 1082.

The rf field consists of a standing wave and a running wave and may be written

$$H(t)=\tfrac{1}{2}H_0e^{i(\omega_0t-kz)}+(\tfrac{1}{2}H_0+H_1)e^{i(\omega_0t+kz)}. \quad (76)$$

H_0 is the amplitude of the standing wave and H_1 is that of the running wave. The spectral density $J(\omega)$ is the Fourier transform of the autocorrelation function $G(\tau)$, which is

$$\begin{aligned}G(\tau)&=\langle H(t)H^*(t+\tau)\rangle_{\rm av}\\&=\{\tfrac{1}{2}H_0)^2\langle\exp[ik(z-z')]\rangle_{\rm av}\\&\quad+(\tfrac{1}{2}H_0+H_1)^2\langle\exp[ik(z-z')]\rangle_{\rm av}\\&\quad+(\tfrac{1}{2}H_0+H_1)\tfrac{1}{2}H_0\langle\exp[ik(z+z')]\rangle_{\rm av}\\&\quad+(\tfrac{1}{2}H_0+H_1)\tfrac{1}{2}H_0\\&\quad\times\langle\exp[-ik(z+z')]\rangle_{\rm av}\}\exp[-\gamma|\tau|]. \quad (77)\end{aligned}$$

If τ is large compared with t_0, the mean collision time, z and z', the position of the atom at time t and $(t+\tau)$, respectively, are independent. Since $J(\omega)$ is only of interest near the center of the spectrum, i.e., $\omega-\omega_0\ll t_0^{-1}$, the short time correlations can be neglected so that z and z' can be considered independent.

To simplify the calculation, the variation of field transverse to the axis of the cavity is neglected, and the bulb, which has a radius a, is treated as if it were one dimensional. If the center of the bulb is located at the center of the rf cavity, $z=0$, then a uniform density of the atom in the bulb is described by the distribution function $P(z)=1/2a$. If the atoms enter the bulb at one end and are relaxed uniformly throughout the bulb, the distribution is no longer uniform. In this case the distribution is approximately

$$P(z)=(1/2a)(1+z/na). \quad (78)$$

Here n is the mean number of collisions the atoms make before relaxing. If Eq. (78) is substituted in Eq. (77), the following result is obtained after some manipulation

$$G(\tau)=\left[H_0^2\frac{\sin^2(ak)}{(ak)^2}+2H_0H_1\left\{\frac{\sin^2ak}{(ak)^2}+i\frac{\sin(ak)}{(ak)}\times\frac{1}{n}\left(\frac{\cos(ka)}{(ka)}+\frac{\sin(ka)}{(ka)^2}\right)\right\}\right]\exp[-i\omega_0\tau-\gamma|\tau|]. \quad (79)$$

The imaginary part of $G(\tau)$ represents a frequency shift. This shift is obtained by evaluating $J(\omega)$, the Fourier transform of Eq. (79), and finding the position of the maximum of $J(\omega)$. Assuming $ak<1$, and using the relation $H_0/H_1=2Q_T/T_1$, where Q_T is the coupling Q, one obtains

$$\frac{\omega-\omega_0}{\omega_0}=\frac{2a}{3ln}\frac{1}{Q_TQ_l}. \quad (80)$$

The length of the resonant cavity is l.

As a numerical example, if $n=10^4$, $a/l=0.3$, $Q_T=10^4$, $Q_l=10^9$, the result is $(\omega-\omega_0)/\omega_0=2\times10^{-18}$. This is clearly a negligible effect.

A quantum mechanical treatment of this problem indicates that saturation does not appreciably affect this result, so that the first-order Doppler shift can be completely neglected as a source of frequency shift.

C. Second-Order Doppler Effect

The second-order Doppler effect does not average in the same manner as the first-order effect because of its dependence on the square of its velocity. The fractional shift introduced by this effect is

$$\frac{\omega-\omega_0}{\omega_0}=-\frac{1}{2}\frac{v^2}{c^2}=-\frac{3}{2}\frac{kT}{mc^2}, \quad (81)$$

where m is the mass of the atom, k is Boltzmann's constant, and T is the temperature. The fractional shift is seen to be the ratio of the thermal energy to the rest energy of the atom. For hydrogen its magnitude is $(\omega-\omega_0)/\omega_0=-3\times10^{-13}/°\text{K}$. The shift is three times smaller for tritium.

D. Cavity Pulling

The influence of the cavity tuning on the resonance has been discussed in Sec. II-C. It was shown there that a mistuning of the cavity by an amount $\omega_c-\omega_0$ shifts the frequency by an amount

$$\frac{\omega-\omega_0}{\omega_0}=\frac{\omega_c-\omega_0}{\omega_0}\frac{Q_c}{Q_l}, \quad (27)$$

where Q_c is the quality factor of the cavity. For a ratio Q_c/Q_l of 10^{-6}, and for a fractional shift no larger than 10^{-13}, the cavity must be tuned to approximately 100 cps. For this reason the cavity must be accurately tuned, and either temperature controlled or thermally compensated to a high degree.

E. Zeeman Effect

The second-order magnetic field dependence of the $(F=1, m=0)\rightarrow(F=0, m=0)$ transition is given by

$$\nu=\nu_0+2750H^2 \text{ cps}, \quad (82)$$

where H is in oersted. The fractional shift in frequency due to ΔH, a small change in the field, is

$$(\nu-\nu_0)/\nu_0=3.9\times10^{-6}H\Delta H. \quad (83)$$

A fractional shift of 10^{-13} requires $H\Delta H\cong3\times10^{-8}$ or, for example, a field of 1 moe held constant to 3%. Although this represents a high degree of field stability, the use of the field dependent transitions in the maser to stabilize the magnetic field greatly simplifies the problem.

F. Effect of Neighboring States

The presence of atoms in other than $(F=1, m=0)$ can cause a change in the permeability of the cavity

and thereby shift the resonance. The only states which make appreciable contributions to this are ($F=1$, $m=1$) and ($F=1$, $m=1$). The pulling effect of these states is very small, however, for the following reasons: Normally these states do not couple to the resonant mode because the static magnetic field is parallel, rather than perpendicular, to the oscillating field. In addition, the two states have effects of opposite sign, so that if care is taken to populate them equally they will have a negligible net effect even if the static magnetic field is not precisely parallel to the oscillating field.

ACKNOWLEDGMENTS

The authors wish to express appreciation to E. M. Purcell for his helpful comments on the analysis and interpretation of random relaxation mechanisms and to G. B. Kistiakowsky for an informative conversation on the role of surface reactions. In addition, they wish to thank H. Berg for many useful comments on the paper, and N. Fortson and E. Recknagel for helpful conversations. Numerical calculations were carried out by B. S. Mathur. One of the authors (H.M.G.) wishes to thank the National Science Foundation for a Predoctoral Fellowship during the course of this work.

PHYSICAL REVIEW VOLUME 126, NUMBER 2 APRIL 15, 1962

Angular Distribution of Relativistic Atomic K-Shell Photoelectrons*

T. A. WEBER
Institute for Atomic Research and Department of Physics, Iowa State University, Ames, Iowa

AND

C. J. MULLIN
University of Notre Dame, Notre Dame, Indiana

(Received December 7, 1961)

Using the high-energy limit of the exact Coulomb wave function for the outgoing electron, the differential cross section, correct to three orders in αZ, is calculated for the K-shell photoeffect. An analytic expression, exact in αZ, is obtained for the differential cross section for the special case in which the electron emerges in the forward direction.

I. INTRODUCTION

USING the first Born approximation, Gavrila[1] calculated the differential and total cross sections for the K-shell photoeffect to two orders in αZ. It is apparent from Gavrila's work that the αZ correction is significant even for fairly small values of Z. More recently Pratt[2] made numerical calculations of the total cross section using the high-energy limit of the exact Coulomb wave function for the ejected electron. Pratt also derived an approximation formula which gives the total cross section as a function of Z. This formula compares favorably with the exact numerical results for all values of Z.

In this paper, the differential cross section for the relativistic K-shell photoeffect is calculated by using the high-energy limit of the exact Coulomb wave function for the ejected electron. While this result is correct to three orders in αZ (i.e., to terms of relative order α^2Z^2), it is not a strict expansion in this parameter. We have used Pratt's work as a guide to determine what factors should be left unexpanded. Upon integration over the solid angles of the outgoing electron we then obtain precisely Pratt's approximate formula for the total cross section. One might then conjecture that our result would give an accurate approximate formula for the angular distribution. However, in the forward direction the terms of relative order 1 and αZ vanish, and the resulting cross section is valid only to the first nonvanishing order in αZ. This nonvanishing term makes a contribution of relative order α^2Z^2 to the total cross section. Since the terms of relative order α^2Z^2 make a very small contribution to Pratt's expression for the total cross section, we cannot use a comparison with Pratt's result for the total cross section to justify the validity of our differential cross section for electron ejection angles near the forward direction. Therefore, for this special case of photoelectrons emerging in the forward direction, we calculate the differential cross section correct to all orders in αZ.

Figure 1 shows the angular distribution of the ejected photoelectrons. Figure 2 gives the differential cross section exact in αZ for the special case of forward emission as a function of Z.

II. MATRIX ELEMENT

Neglecting radiative corrections, the matrix element for the photoeffect is

$$M=-\left(\frac{2\pi\alpha}{k}\right)^{\frac{1}{2}}\int\psi_2^*\boldsymbol{\alpha}\cdot\boldsymbol{\varepsilon}e^{i\mathbf{k}\cdot\mathbf{r}}\psi_1(\mathbf{r})d\mathbf{r}, \quad (1)$$

* Contribution No. 1085. Work was supported in part by the U. S. Atomic Energy Commission.

[1] M. Gavrila, Phys. Rev. **113**, 514 (1959).

[2] R. H. Pratt, Phys. Rev. **117**, 1017 (1960).